

## Supporting Information

### Three *in situ* - synthesized novel inorganic-organic hybrid materials based on metal (M = Bi, Pb) iodide and organoamine using one-pot reactions: structures, band gaps and optoelectronic properties

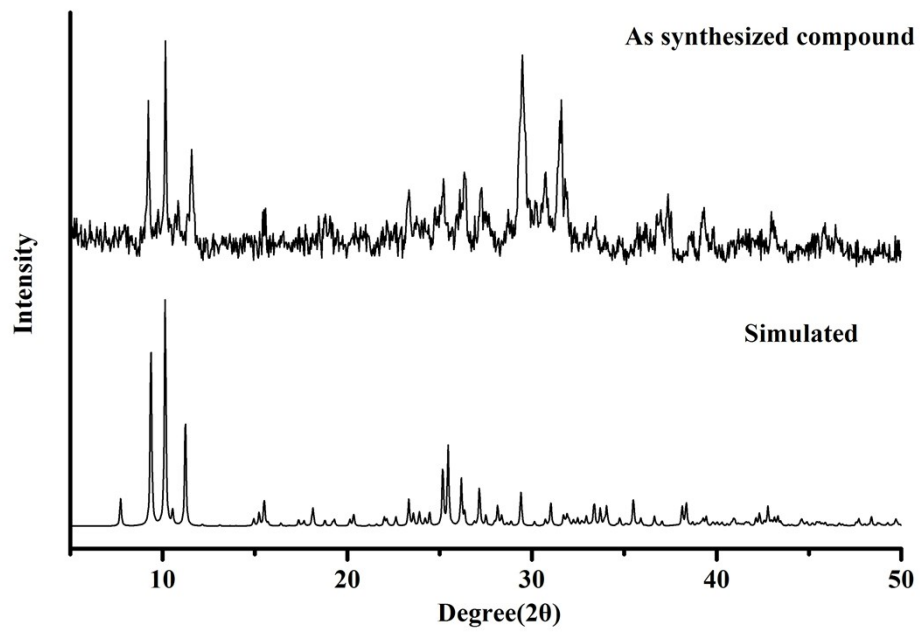
Zhi Shuo Yan,<sup>a</sup> Ji Ying Long,<sup>a</sup> and Yun Gong<sup>\*a</sup>

<sup>a</sup> *Department of Applied Chemistry, College of Chemistry and Chemical Engineering, Chongqing University, Chongqing 400044, P. R. China Tel: +86-023-65106150 E-mail: gongyun7211@cqu.edu.cn*

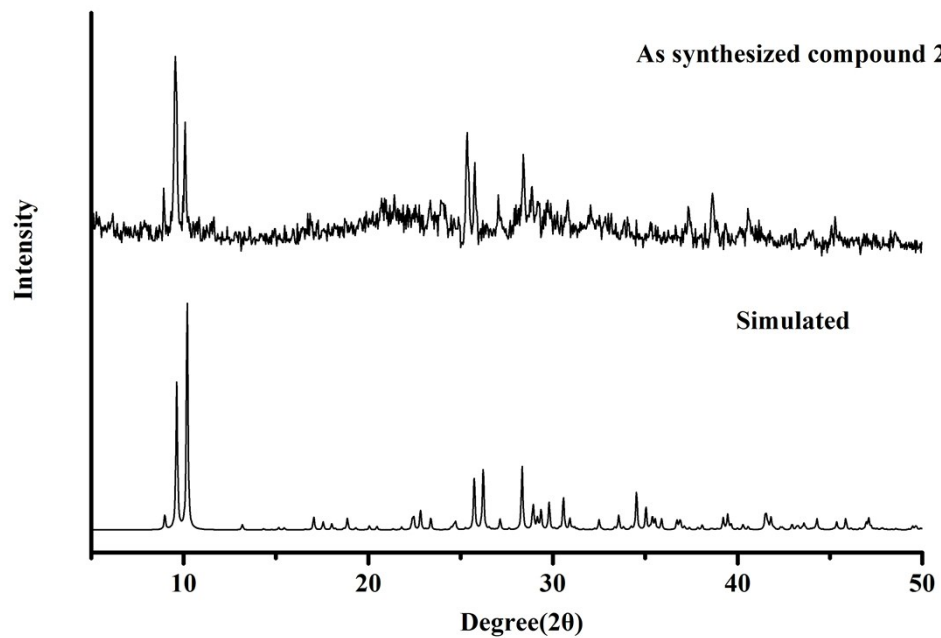
#### Experimental

**Synthesis of perovskite CH<sub>3</sub>NH<sub>3</sub>PbI<sub>3</sub>.** CH<sub>3</sub>NH<sub>3</sub>PbI<sub>3</sub> was prepared according to the previous literature.<sup>1-3</sup> There are two main steps to prepare CH<sub>3</sub>NH<sub>3</sub>PbI<sub>3</sub>. (i) Methylammonium iodide (CH<sub>3</sub>NH<sub>3</sub>I) powder was synthesized by mixing 30 mL of methylamine (35-40 wt % in aqueous solution) and 23.3 mL of hydroiodic acid (48 wt % in aqueous solution) in 250 mL single-necked round-bottom flask at 0 °C for 2 h with intense stirring. Then the precipitate was collected by using a rotary evaporator through carefully removing the solvents at 60-70 °C. After cooling to room temperature, the pale yellow raw products of CH<sub>3</sub>NH<sub>3</sub>I were precipitated from mother solution. In order to obtain the fine CH<sub>3</sub>NH<sub>3</sub>I powder, the raw powder can be dissolved in absolute ethanol by stirring for 30 min and then recrystallized with diethyl ether. The washing step was repeated three times. The final products were collected by a Buchner funnel and dried at 60 °C in a vacuum oven for 24 h.<sup>1, 2</sup> (ii) CH<sub>3</sub>NH<sub>3</sub>PbI<sub>3</sub> was synthesized from a stoichiometric reaction between the commercial PbI<sub>2</sub> (99%) and the obtained fine CH<sub>3</sub>NH<sub>3</sub>I powder, in detail, CH<sub>3</sub>NH<sub>3</sub>I (0.01mmol) and PbI<sub>2</sub> (0.01mmol) were dissolved in 10 mL in absolute ethanol at 70 °C with energetic stirring for 30 min, then the solution was left to room temperature for cooling naturally, the brown dark crystals CH<sub>3</sub>NH<sub>3</sub>PbI<sub>3</sub> can be crystallized. The crystals were isolated by filtration and then dried under reduced pressure.<sup>3</sup>

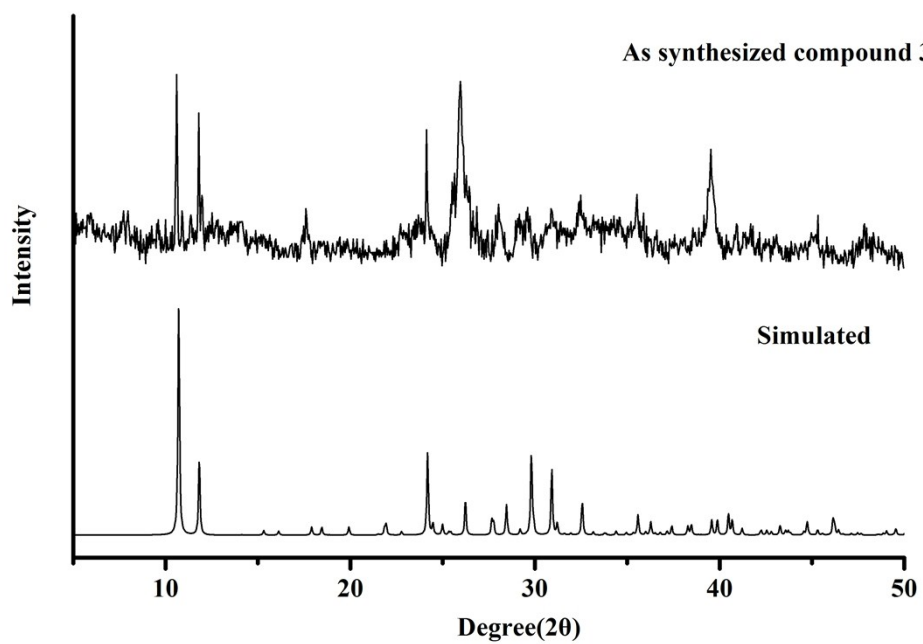
(a)



(b)



(c)



(d)

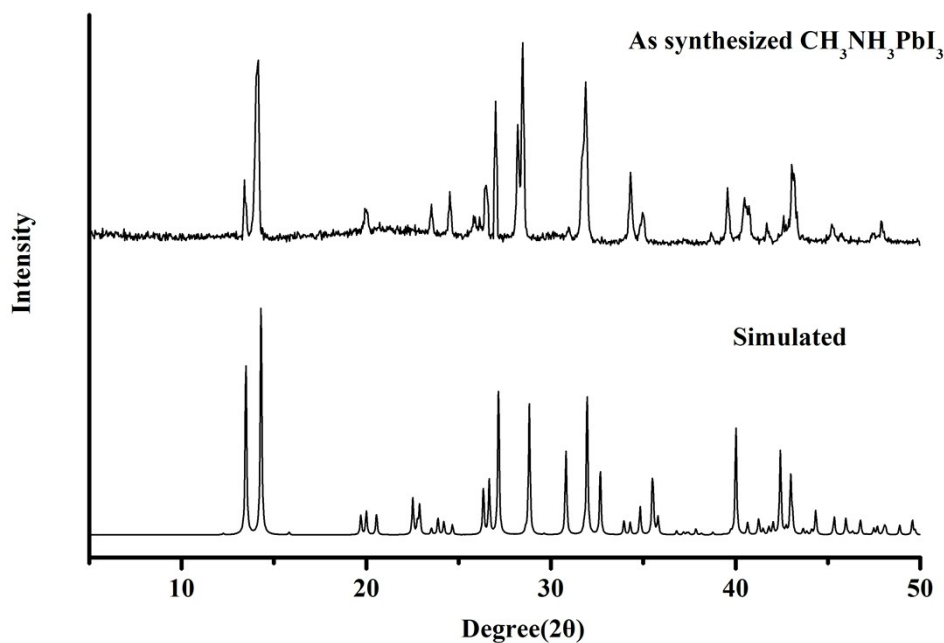


**Fig. S1** Powder X-ray diffraction (PXRD) patterns for compounds **1** (a), **2** (b), **3** (c) and  $\text{CH}_3\text{NH}_3\text{PbI}_3$  (d).

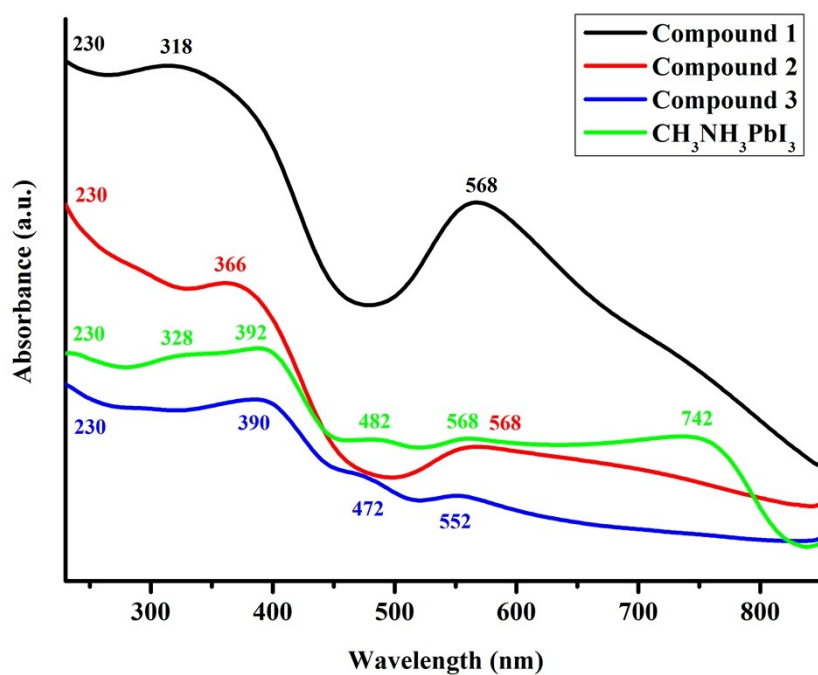


**Fig. S2** UV-vis absorption spectra for compounds **1-3** and  $\text{CH}_3\text{NH}_3\text{PbI}_3$  in the solid state at room temperature.

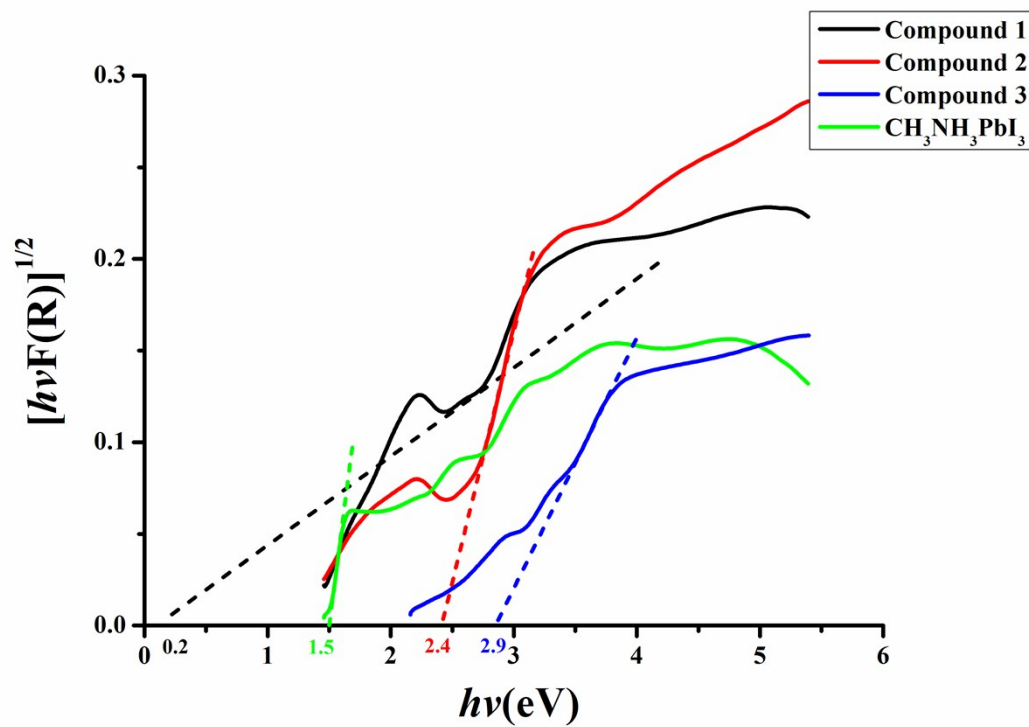


**Fig. S3** The diffuse reflectance spectra of compounds **1-3** and the perovskite  $\text{CH}_3\text{NH}_3\text{PbI}_3$  in Kubelka-Munk functions.

The diffuse reflectance spectra of compounds **1-3** and the perovskite  $\text{CH}_3\text{NH}_3\text{PbI}_3$  are shown in **Fig. S3**. The relationship between the absorption coefficient and band gap  $E_{\text{gap}}$  for an indirect semiconductor can be determined by the equation:

$$\alpha E \approx A_1(E - E_{\text{gap}})^2 \quad (1)$$

Where  $E = h\nu$  is the photon energy,  $A_1$  is a constant.

$F(R)$  is the Kubelka–Munk equation, which can be described as:

$$F(R) = (1-R)^2/2R = k/s \quad (2)$$

Where  $R$  is the experimental value in reflectance of the sample,  $k$  is the molar absorption coefficient, and  $s$  is the scattering coefficient, From eqs 1 and 2, the following eq 3 can be drawn:

$$[h\nu F(R)]^{1/2} = A_2[h\nu - E_{\text{gap}}] \quad (3)$$

According to the plot of  $[h\nu F(R)]^{1/2}$  vs  $h\nu$ , the value of band gap  $E_{\text{gap}}$  of the sample can be obtained by extrapolating the linear fitted region to  $[h\nu F(R)]^{1/2} = 0$ .

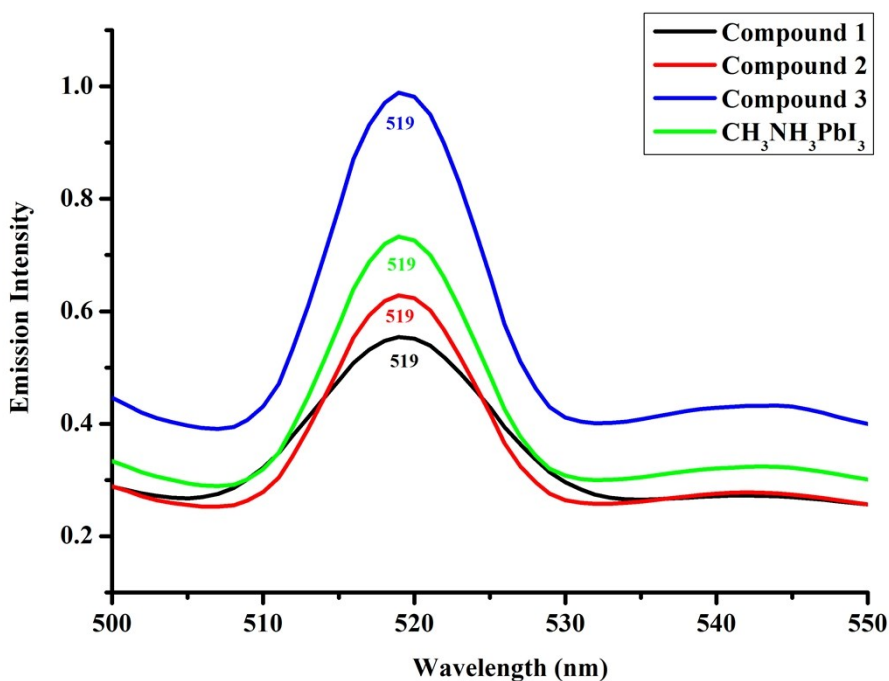


**Fig. S4** The emission spectra of compounds **1-3** and  $\text{CH}_3\text{NH}_3\text{PbI}_3$  in the solid state at room temperature.

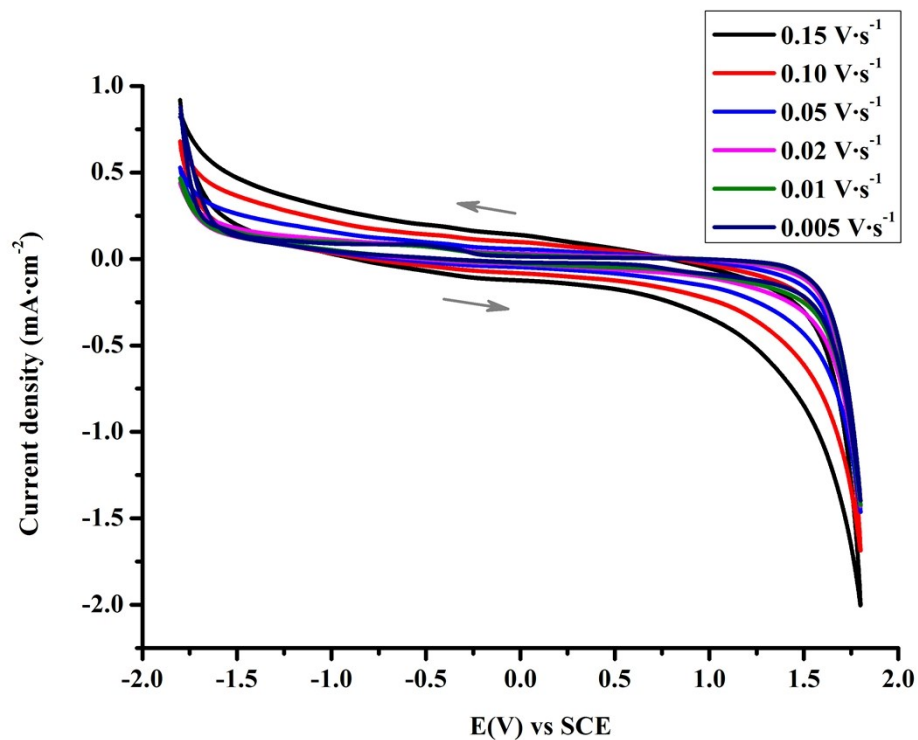
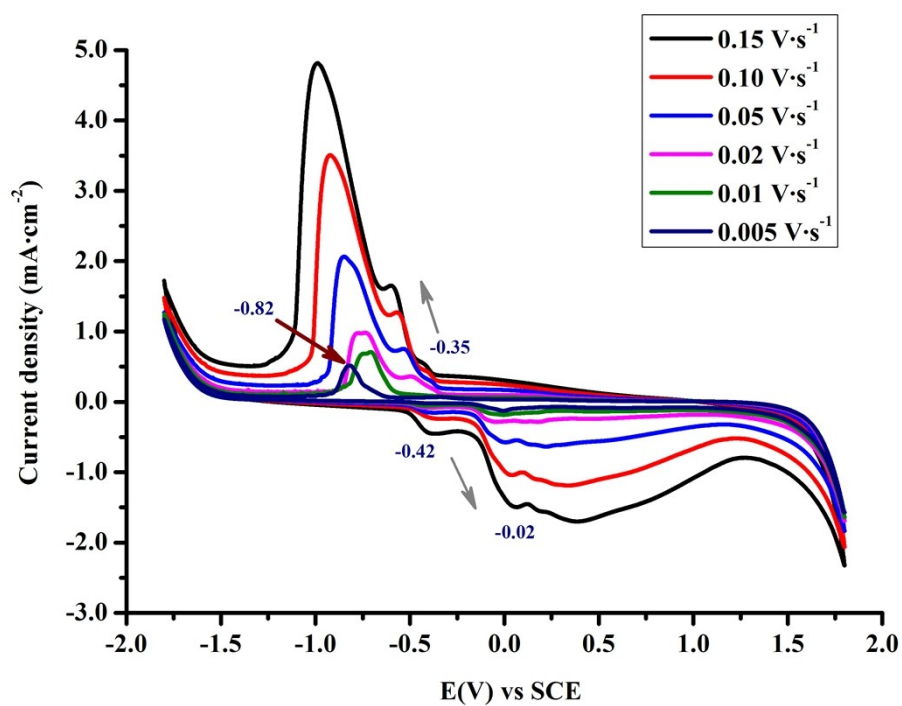


**Fig. S5** CVs of the bare GCE in neutral sodium sulfate aqueous solution (0.2 M, 50 mL) at different sweep rates (scan directions denoted in black arrows).

(a)



(b)

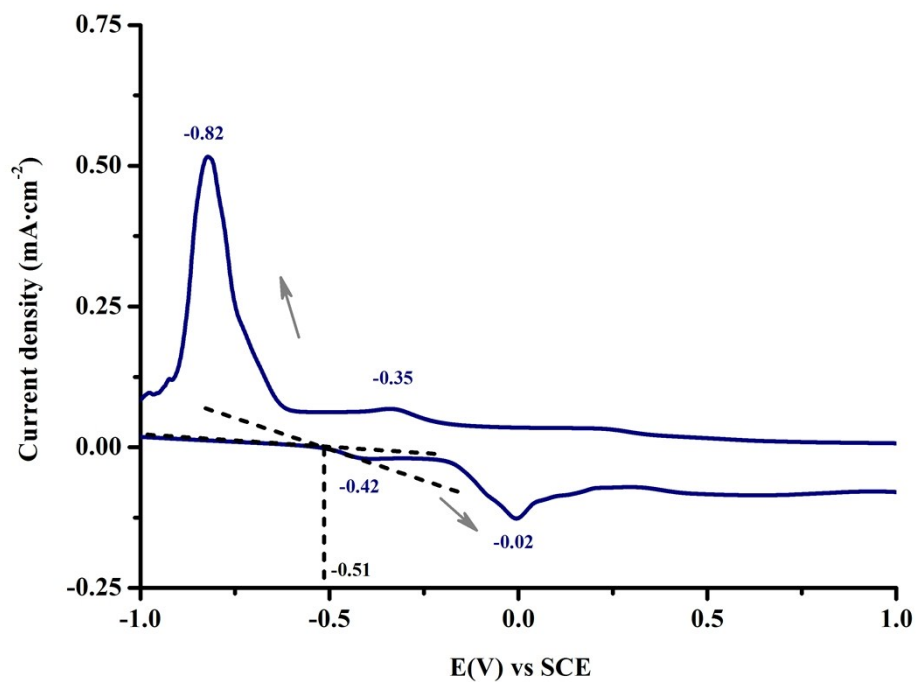
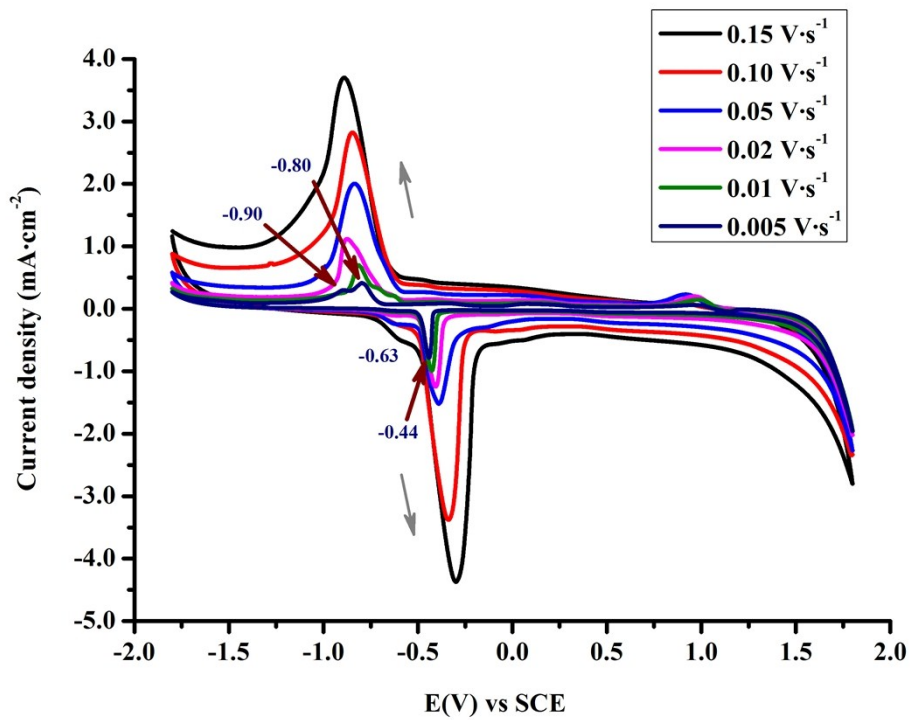


**Fig. S6** CVs of **1-GCE** in neutral sodium sulfate aqueous solution (0.2 M, 50 mL) at different sweep rates (The redox couples at the scan rate of  $0.005 \text{ V}\cdot\text{s}^{-1}$  denoted in purple) **(a)**; The onset potential calculated for the first oxidation peak at the scan rate of  $0.005 \text{ V}\cdot\text{s}^{-1}$  at **1-GCE** **(b)** (scan directions denoted in black arrows).

(a)



(b)

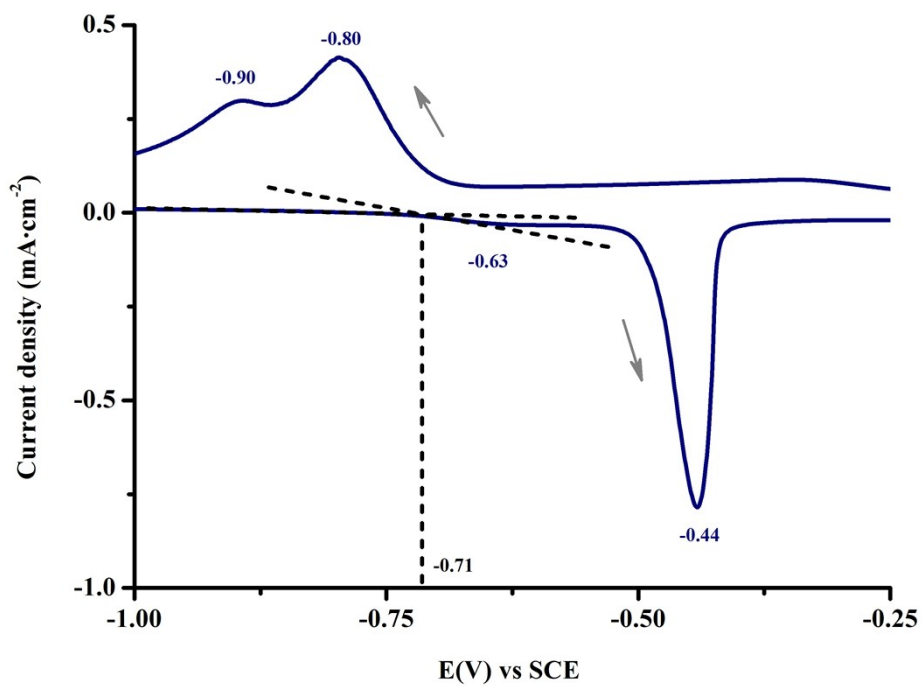
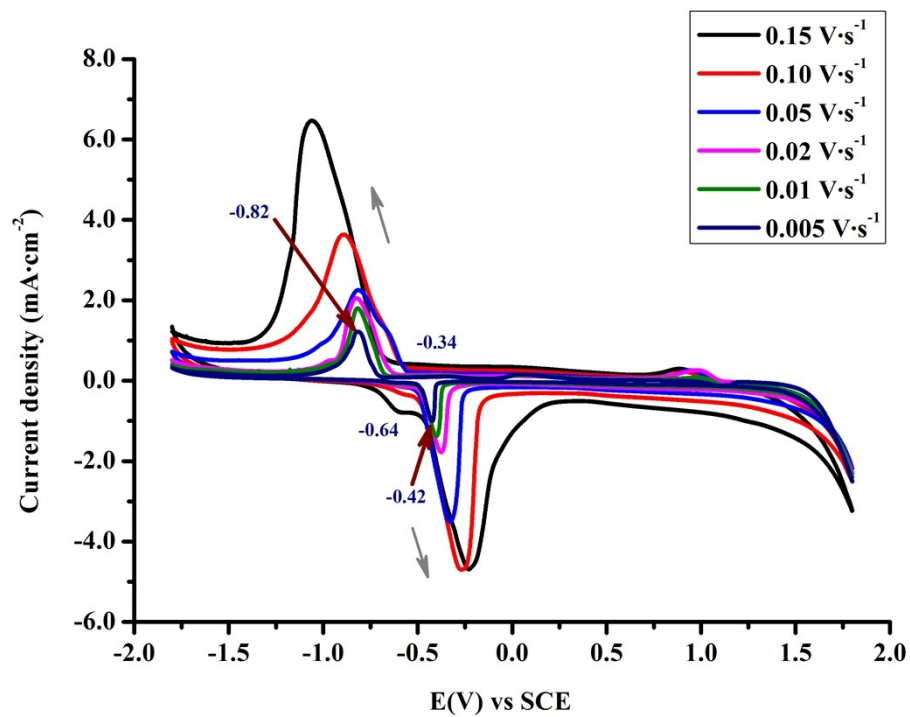


**Fig. S7** CVs of 2-GCE in neutral sodium sulfate aqueous solution (0.2 M, 50 mL) at different sweep rates (The redox couples at the scan rate of  $0.005 \text{ V}\cdot\text{s}^{-1}$  denoted in purple) (a); The onset potential calculated for the first oxidation peak at the scan rate of  $0.005 \text{ V}\cdot\text{s}^{-1}$  at 2-GCE (b) (scan

directions denoted in black arrows).

(a)



(b)

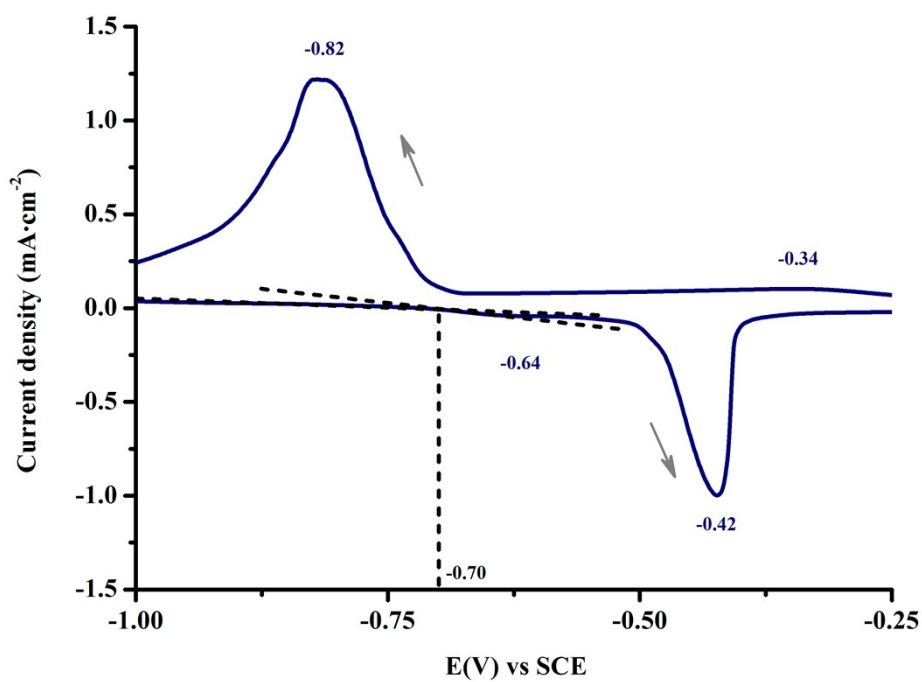
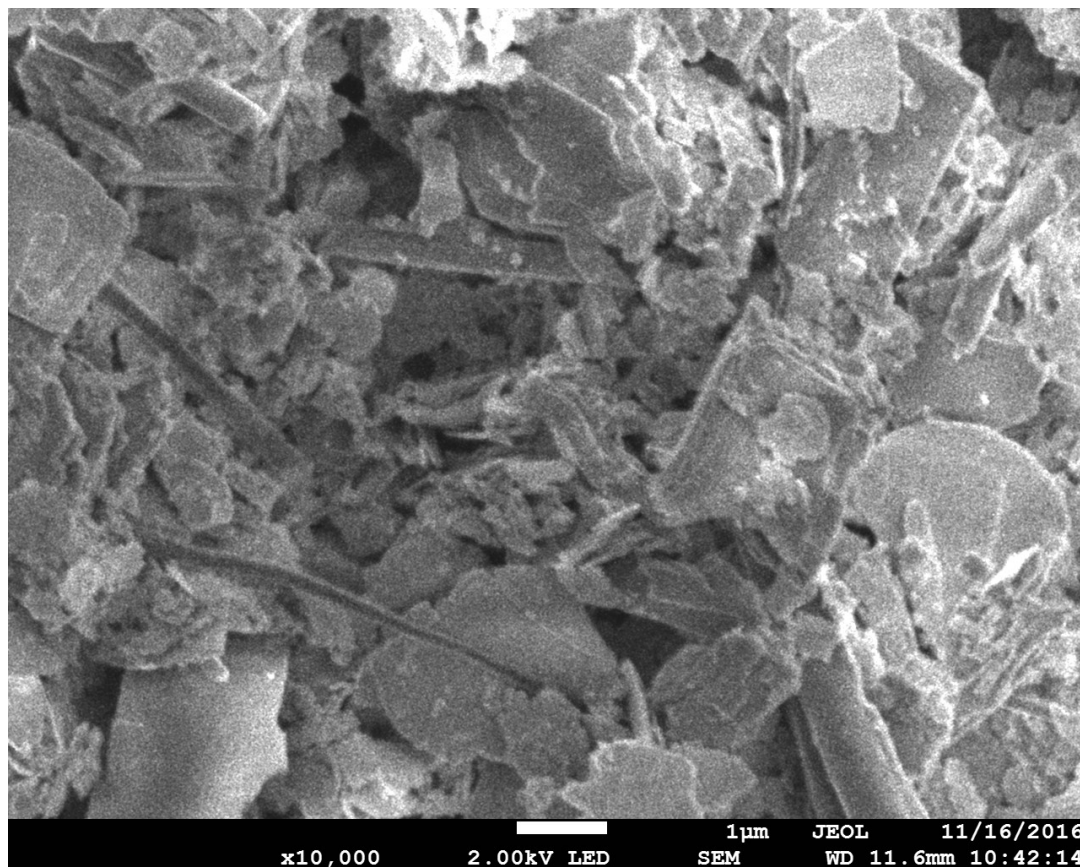
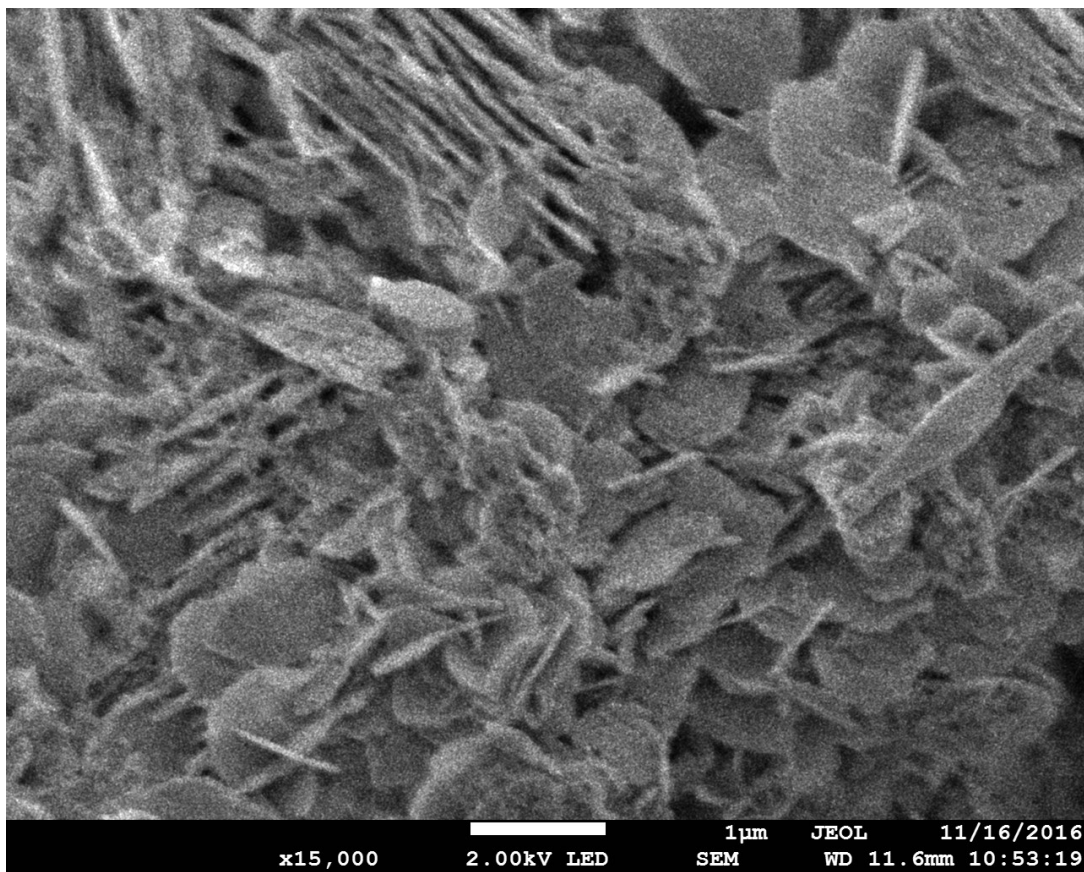


**Fig. S8** CVs of **3-GCE** in neutral sodium sulfate aqueous solution (0.2 M, 50 mL) at different sweep rates (The redox couples at the scan rate of  $0.005 \text{ V}\cdot\text{s}^{-1}$  denoted in purple) **(a)**; The onset potential calculated for the first oxidation peak at the scan rate of  $0.005 \text{ V}\cdot\text{s}^{-1}$  at **3-GCE** **(b)** (scan directions denoted in black arrows).

**(a)**



**(b)**



(c)

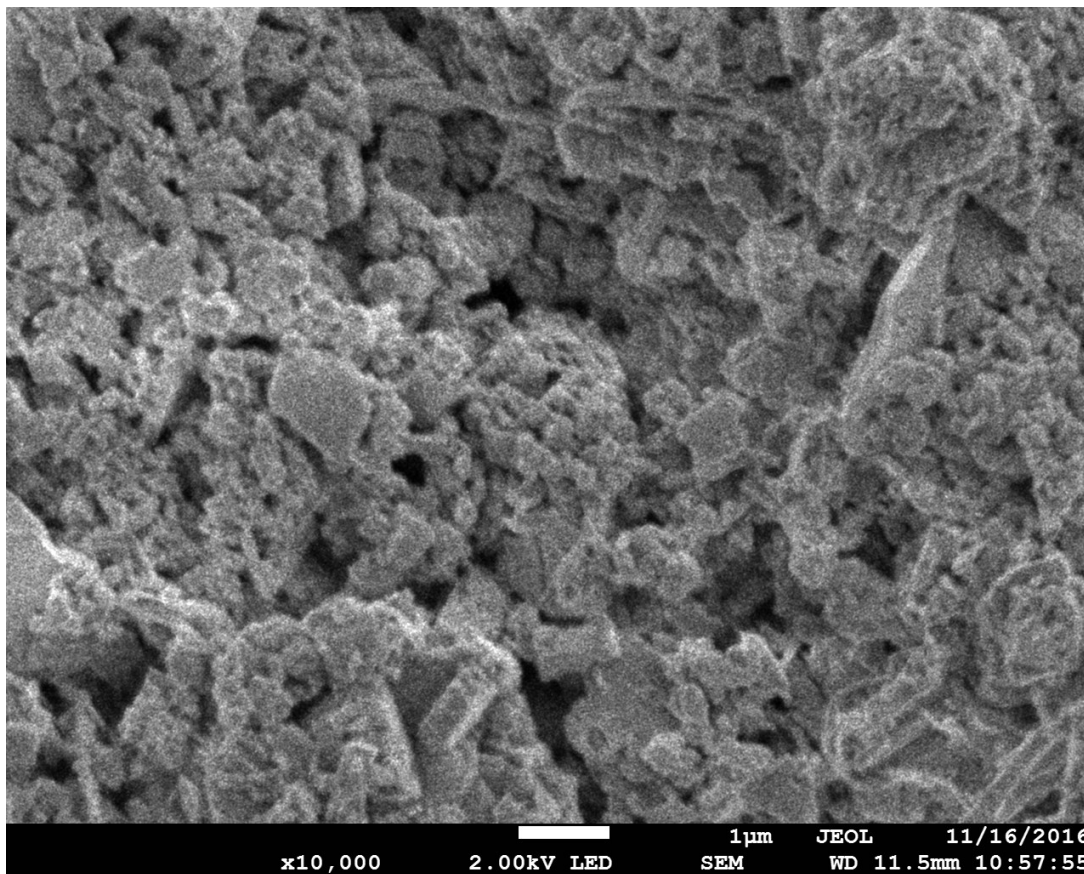


Fig. S9 The top-view SEM images of compounds 1 (a), 2 (b) and 3 (c) on the surface of FTO

slices.

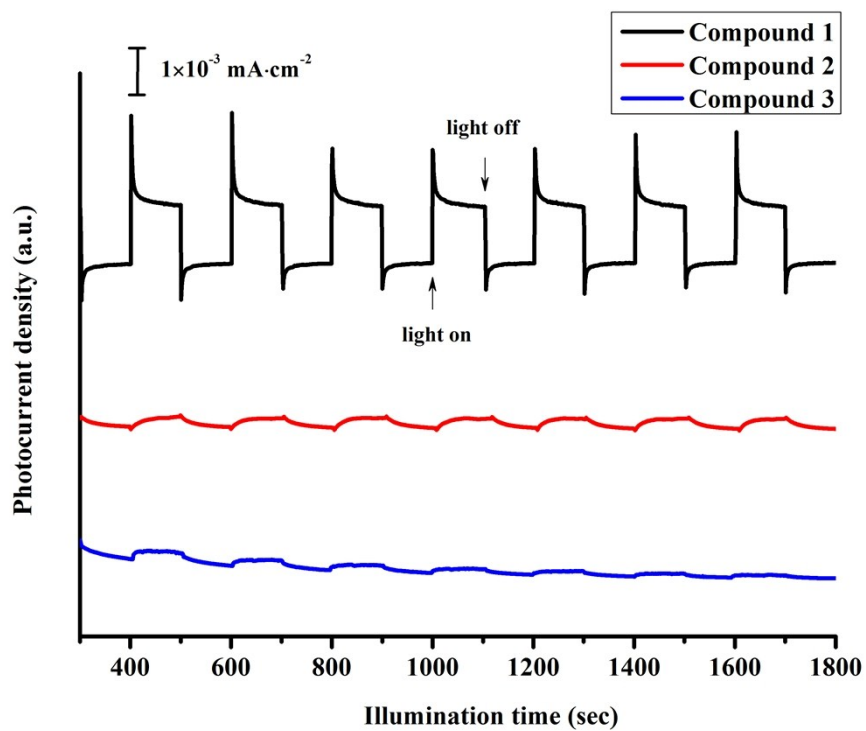


Fig. S10 The transient photocurrent responses of compounds 1-3.

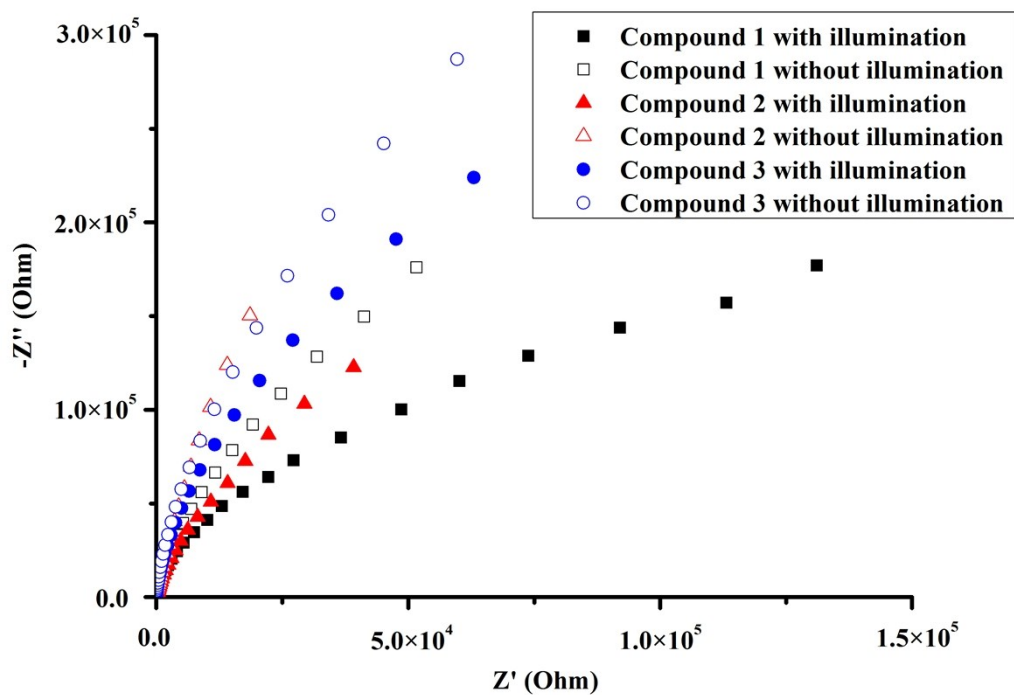
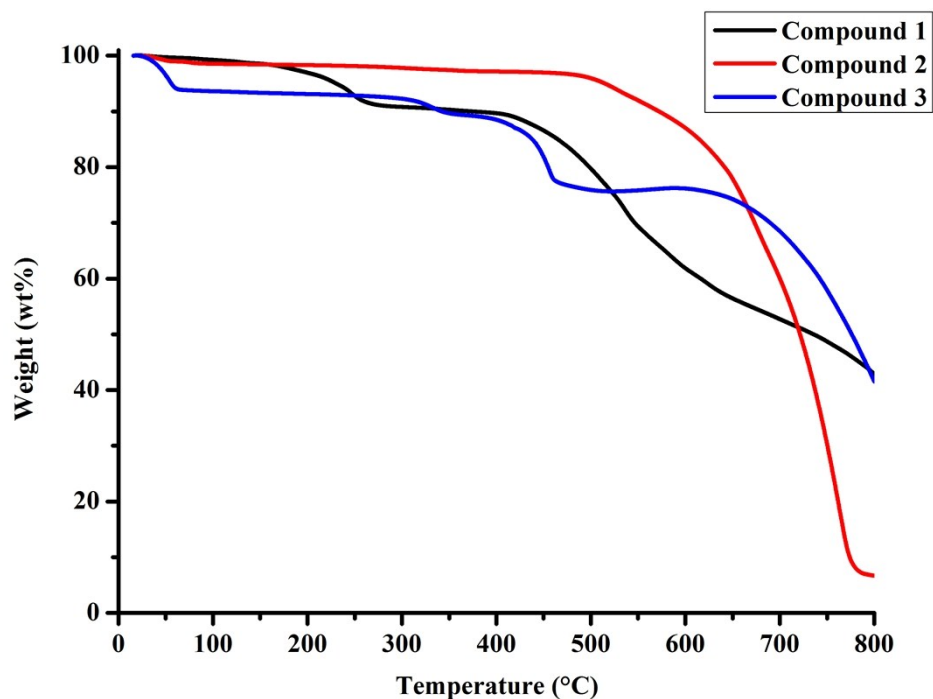


Fig. S11 Nyquist plots ( $Z'$  vs  $-Z''$ ) of the three-electrode systems at  $E = 0 \text{ V}$  vs Ag/AgCl in neutral

sodium sulfate aqueous solution (0.2 M, 50mL) in the absence and presence of visible light illumination ( $350\text{ nm} < \lambda < 650\text{ nm}$ ) with **1-3** @ FTO as the working electrode, respectively.



**Fig. S12** Thermogravimetric analyses (TGA) curves for compounds **1-3**.

## References

1. W. J. Ke, G. J. Fang, J. Wang, P. L. Qin, H. Tao, H. W. Lei, Q. Liu, X. Dai and X. Z. Zhao, *ACS Appl. Mater. Interfaces*, 2014, **6**, 15959.
2. S. S. Chen, L. Lei, S. W. Yang, Y. Liu and Z. S. Wang, *ACS Appl. Mater. Interfaces*, 2015, **7**, 25770.
3. D. Cui, Z. Yang, D. Yang, X. D. Ren, Y. C. Liu, Q. B. Wei, H. B. Fan, J. H. Zeng and S. Z. Liu, *J. Phys. Chem. C*, 2016, **120**, 42.